ChemPubSoc Europe

DOI: 10.1002/chem.201705307

CHEMISTRY
A European Journal
Communication

Hypervalent Complexes

Detection of Indistinct Fe–N Stretching Bands in Iron(V) Nitrides by Photodissociation Spectroscopy

Erik Andris,[a] Rafael Navrátil,[a] Juraj Jašík,[a] Gerard Sabenya,[b] Miquel Costas,*[b] Martin Srnec,*[c] and Jana Roithová*[a]

Abstract: We report for the first time infrared spectra of three non-heme pseudo-octahedral iron(V) nitride complexes with assigned Fe–N stretching vibrations. The intensities of the Fe–N bands in two of the complexes are extremely weak. Their detection was enabled by the high resolution and sensitivity of the experiments performed at 3 K for isolated complexes in the gas phase. Multireference CASPT2 calculations revealed that the Fe–N bond in the ground doublet state is influenced by two low-lying excited doublet states. In particular, configuration interaction between the ground and the second excited state leads to avoided crossing of their potential energy surfaces along the Fe–N coordinate, which thus affects the ground-state Fe–N stretching frequency and intensity. Therefore, DFT calculated Fe–N stretching frequency strongly depends on the amount of Hartree–Fock exchange potential. As a result, by tuning the amount of Hartree–Fock exchange potential in the B3LYP functional, it was possible to obtain theoretical spectra perfectly consistent with the experimental data. The theory shows that the intensity of the Fe–N stretching vibration can almost vanish due to strong coupling with other stretching modes of the ligands.

A diverse set of challenging oxidation reactions catalysed by iron-containing enzymes in nature has motivated studies on high-valent compounds featuring Fe–O and Fe–N bonds.[1–5] The spectroscopic data on iron-oxo compounds, including the Fe–O stretching frequency, are well established;[6,7] however, the information about Fe–N bonds is still scarce. Spectral signatures of the Fe–N bond depend on both the oxidation state of iron centre and the symmetry of the surrounding ligand field.[8] In the case of iron(V) nitrides (d^3 configuration), orbital splitting in trigonal C_{3v} ligand field allows the accommodation of all three electrons in orbitals having the non-bonding character relative to the Fe–N bond.[9] This results in a relatively strong–and thus unreactive–bond with $\tilde{\nu}$(FeN) of $\approx$1000 cm^{-1}.[10,11]

Conversely, the octahedral C_{4v} ligand field can accommodate only two electrons in a non-bonding orbital (d_{xy}), and the remaining electron occupies the antibonding π*(Fe–N) orbital. This should make the Fe–N bond weaker and more reactive. The Fe–N stretching frequencies of three porphyrin complexes were determined by resonance Raman spectroscopy and they were found around 870 cm^{-1}.[12] All other attempts to detect the Fe–N transitions have failed, presumably due to their low IR intensities.[13,14] Alternatively, ^{57}Fe nuclear resonance vibrational spectroscopy (NRVS)[15] can be used. It was used to determinate the Fe–N vibration frequency in [(cyclam-ac)FeN]$^+$ (**1**; cyclam-ac = 1,4,8,11-tetraazacyclotetradecane-1-acetate; $\tilde{\nu}$ = 864 cm^{-1}).[13] The drawback of NRVS spectroscopy is that it requires the use of synchrotron radiation and ^{57}Fe-enriched compounds. Therefore, finding a more convenient, simpler and faster method to characterize these compounds has remained a challenging task. In this study, we successfully used helium-tagging infrared photodissociation (IRPD) spectroscopy[16,17] to overcome the high thermal instability and weakness of the IR absorption of these iron(V) nitrides.

The studied complexes were prepared from their iron(III) azide precursors by nitrogen elimination during the electrospray ionization (ESI) process, as previously reported.[18–23] The generation of such reactive ions in the gas phase at low pressures precludes any unwanted bimolecular reactions, which usually hamper the investigation of these compounds in the condensed phase.

Firstly, we measured the IR spectrum of **1**. Complex **1** shows a clearly visible Fe–N stretch at 855 cm^{-1} that redshifts to 834 cm^{-1} upon ^{15}N labelling (Figure 1 a). The shift is consistent with the prediction for the Fe–N diatomic oscillator (832 cm^{-1}). Note that the IRPD value of 855 cm^{-1} is slightly lower than the NRVS value of 864 cm^{-1} observed in the condensed phase (the NRVS spectrum was measured in a matrix containing counter ions and solvent). The experimental spectrum agrees well with the theoretical spectrum of the doublet ground state of **1**.[24]

[a] E. Andris, R. Navrátil, Dr. J. Jašík, Prof. J. Roithová
Department of Organic Chemistry, Faculty of Science
Charles University, Hlavova 2030/8, 128 43 Prague 2 (Czech Republic)
E-mail: roithova@natur.cuni.cz

[b] G. Sabenya, Prof. M. Costas
Departament de Quimica and Institute of Computational Chemistry and Catalysis (IQCC), University of Girona
Campus Montilivi, Girona 17071 (Spain)
E-mail: miquel.costas@udg.edu

[c] Dr. M. Srnec
J. Heyrovsky Institute of Physical Chemistry of the CAS, v. v. i.
Dolejškova 2155/3, 182 23 Prague 8 (Czech Republic)
E-mail: martin.srnec@jh-inst.cas.cz

Supporting information and the ORCID identification number for the author of this article can be found under https://doi.org/10.1002/chem.201705307.

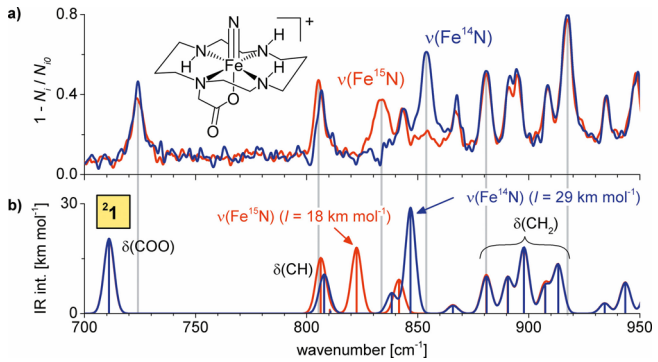

Figure 1. a) Infrared photodissociation spectra of **1**. Blue and red traces correspond to ^{14}N and ^{15}N isotopomers, respectively. b) DFT predictions of the IR spectra of the doublet ground state of **1** calculated at the B3LYP-16.3HFX-D3/6–311 + G** level of theory (scaling factor: 0.99). Predictions of other spin isomers and isomers with oxidized ligand are in Figure S5.

Comparison with other spin states and other isomers of **1** is in the Supporting information (Figure S5).

Previous studies of **1** in the gas phase reported a complete lack of bimolecular reactivity.[18,19] It was unexpected, because other iron(V) nitrido complexes show profound reactivity.[20,21,23] It was hypothesized that the lack of intermolecular reactivity was due to self-oxidation of **1** and formation of its unreactive isomers. Having confirmed that complex **1** generated in our ion source retains the iron(V) nitrido character, we probed its reactivity with cyclohexadiene. Complex **1** indeed proved to be completely unreactive. Hence, contrary to expectations, iron(V) nitrido complexes are not necessarily highly reactive in the gas phase.

After establishing that our method is suitable for studying the iron(V) nitride **1**, we turned our attention to the $[(Me_2Py_2TACN)FeN]^{2+}$ complex (**2**, Me_2Py_2TACN = 1-(di(pyridin-2-yl) methyl)-4,7-dimethyl-1,4,7-triazacyclononane; preparation of the precursor azide is described in the Supporting information), which does not contain the anionic acetate ligand in the *trans* position to the nitrido group. The IRPD spectrum of **2** is shown in Figure 2a. The Fe–N stretch at 866 cm^{-1} disappears upon ^{15}N labelling, and a weak Fe–^{15}N band emerges at 845 cm^{-1} in accordance with the prediction for the Fe–N oscillator (843 cm^{-1}). In addition, the band at 829 cm^{-1} is slightly redshifted. To make the changes induced by the ^{15}N labelling more visible, subtracted spectra are shown in Figure 2b. Using density functional theory (DFT), we tried to reproduce these spectral changes, which required a correct prediction of both the Fe–N and ligand vibration frequencies. Extensive tests of DFT functionals showed that the calculated Fe–N frequency strongly depends on the amount of Hartree–Fock exchange potential (HFX; Figure S1). Therefore, we varied the amount of HFX in the B3LYP functional (Figures S2 and S10)[25] and found 16.3% HFX for **1** and 17.4% HFX for **2** to fit best the experimental data (Figure 1b and Figures 2c,d). The calculations showed a coupling between the Fe–N and other vibrations of the complex **2** in the same frequency range. Therefore, the isotopic labelling also affects other bands, such as the triazacyclononane deformation band at 829 cm^{-1}.

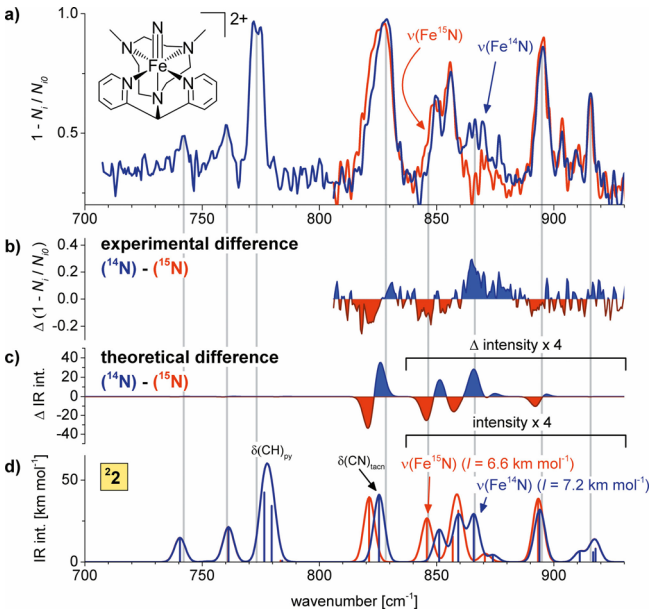

Figure 2. a) Infrared photodissociation spectra of **2**. Blue and red traces correspond to ^{14}N and ^{15}N labelling, respectively. b) Experimental ($^{14}N-^{15}N$) difference spectrum. c,d) Theoretically predicted spectra of the $^{14/15}N$-labelled doublet **2** calculated at the B3LYP-17.4HFX-D3/6–311 + G** level of theory. Frequencies are scaled by 0.99. Predictions of other spin isomers are shown in Figure S6.

We then investigated the recently reported $[(MePy_2TACN)FeN]^{2+}$ complex (**3**, $MePy_2TACN$ = 1-methyl-4,7-bis(2-picolyl)-1,4,7-triazacyclononane) (Figure 3).[23] The differences

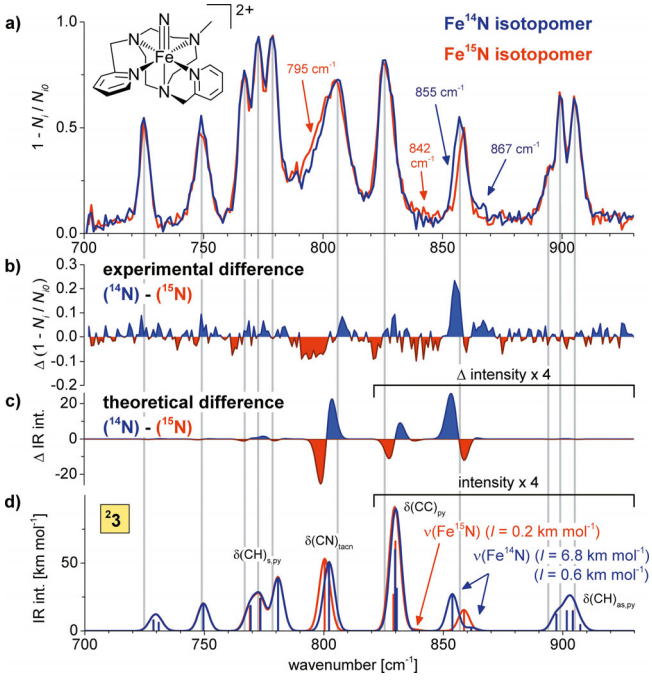

Figure 3. a) Infrared photodissociation spectra of **3**. Blue and red traces correspond to ^{14}N and ^{15}N labelling, respectively. b) Experimental ($^{14}N-^{15}N$) difference spectrum. c,d) Theoretically predicted spectra of the $^{14/15}N$-labelled doublet **3** calculated at the B3LYP-16.3HFX-D3/6–311 + G** level of theory. Frequencies scaled by 0.99. Predictions of other spin isomers are shown in Figure S7.

between the IRPD spectra of ^{14}N- and ^{15}N-labelled **3** (Figure 3b) are relatively small. Nevertheless, upon the ^{15}N labelling, the regions of the bands at 855 and 867 cm^{-1} (indicated by blue arrows in Figure 3a) decreased, and the absorption intensity of the bands at 842 cm^{-1} and 795 cm^{-1} increased. Similarly to complex **2**, the DFT (B3LYP with 16.3% HFX) predicts a coupling between the Fe–N stretching and ligand vibrational modes.

Theory shows that both of the bands at 854 and 862 cm^{-1} have Fe–N stretching character. Only one Fe–N band remains upon ^{15}N labelling (at 839 cm^{-1}) and this band has almost zero intensity (Figure 3d). This is further confirmed when comparing the experimental (Figure 3b) and theoretical (Figure 3c) difference spectra, which show the same changes in band patterns between ^{14}N and ^{15}N labelling. Specifically, the bands with strong Fe–N stretching character in the theoretical spectra (Figure 3d, blue trace) match the features at 855 and 867 cm^{-1} in the experimental spectra (Figure 3a, blue trace). Furthermore, upon ^{15}N labelling, the Fe–N stretching band weakens and redshifts to 842 cm^{-1} (Figure 3a, red trace). The changes observed at the 795 cm^{-1} band (Figure 3) result from the coupling between the Fe–N stretching and a triazacyclononane deformation mode (the same effect was observed for **2**, see above).

We note that the presence of a self-oxidized isobaric complex without the Fe–N moiety was ruled out based on: 1) the chemical reactivity that we reported previously[23] (hydrogen abstraction and alkene aziridination), and 2) the comparison between the spectra of **3** and its iron(III) azide precursor that showed no ligand degradation (Figure S3).

The good agreement between the predicted and observed spectral features of all three nitrides supports our DFT approach. However, this approach is arbitrary due to an empirical calibration of the HFX admixture, relying on error compensation. Thus, in order to further support our approach, we used the ab initio CASSCF/CASPT2 method, which correctly describes the electronic structure and accounts for the expected static correlation effects of iron nitrides.[26] We mostly focused on the comparison between ^{2}**2** and ^{2}**3** because we were unable to find a fully consistent active space for ^{2}**1**.

Our calculations indicated the presence of three relatively low-lying doublet spin states in both nitrides. Therefore, we applied the SA-CASSCF/MS-CASPT2 method to calculate the three lowest-lying potential energy curves along the Fe-N stretching coordinate (Figure 4). The first two of the three electronic states are quasi-degenerate, with the unpaired electron in the d_{xz} or d_{yz} orbital (denoted as $^2\tilde{\mathbf{X}}$ or $^2\tilde{\mathbf{A}}$, respectively) and with the equilibrium Fe–N bond length at approximately 1.65 Å. The third state, $^2\tilde{\mathbf{B}}$, has the unpaired electron in the $d_{x^2-y^2}$ orbital, which results in a stronger Fe–N bond. The avoided crossing between the $^2\tilde{\mathbf{X}}$ and the $^2\tilde{\mathbf{B}}$ state near 1.55 Å indicates their configuration interaction mixing. The degree of this mixing is much larger in the case of ^{2}**3** (≈10 times) as reflected by the energy gap of the avoided crossing.

The self-interaction error can, to some extent, simulate the static correlation effects.[27] This may explain why an increase of this error in the B3LYP functional, introduced by the HFX reduction, can significantly change the position of the stretching Fe–N band. A stronger interaction between the electronic states of ^{2}**3** corresponds to a larger portion of static correlation, which requires a more extensive reduction of the HFX contribution (16.3%) as compared to 17.4% for ^{2}**2** (Figure S4). Moreover, our exploratory calculations indicate a strong interstate coupling in ^{2}**1**, similarly to ^{2}**3**. Therefore, we used the same HFX value for both **1** and **3** (16.3%).

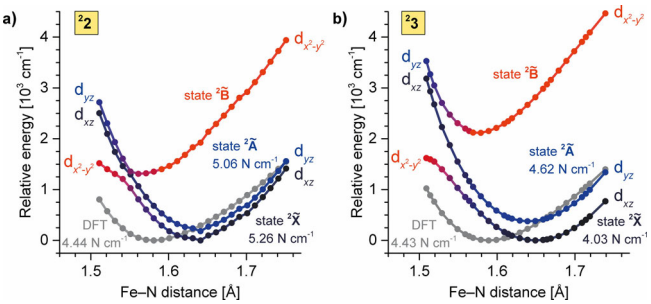

Figure 4. MS-CASPT2 relative energy of the first three electronic states (coloured traces) and DFT relative energy of the ground states (grey traces) on the relaxed potential energy surfaces of: a) ^{2}**2**, and b) ^{2}**3** along the Fe–N stretching coordinate. The geometries were obtained at the same DFT level as used for the results in Figures 2 and 3. The dominant character of each state (labelled according to a singly occupied orbital in the dominant configuration; *z* axis defined along the Fe–N bond vector) is shown next to each trace.

We also tried to extract the Fe–N bond force constants directly from the MS-CASPT2 calculated potential energy curves. The values correspond to the $\tilde{\nu}$(Fe–N) frequencies in the 750–900 cm^{-1} range;[28] however, we were unable to obtain more accurate estimates. Figure 4 shows that the Fe–N bond is longer at the MS-CASPT2 level than at the DFT level. All other coordinates are frozen at the DFT optimum which distorts the explored MS-CASPT2 potential energy curve (see also Figure S11). Notwithstanding, the comparison between Figures 4a and b shows that the strong mixing of the $^2\tilde{\mathbf{X}}$ with the $^2\tilde{\mathbf{B}}$ state translates into a lower experimental Fe–N frequency (≈10 cm^{-1} lower in the case of **3**).

Interestingly, the very low intensity of the Fe–N band, which virtually disappears upon ^{15}N-labelling in case of **3**, was predicted by DFT calculations. This suggests that DFT wave function analysis should provide an explanation for the origin of this low intensity. One possibility is that the low intensity comes from a low polarity of the Fe–N bond. From the natural population analysis,[29] the differences in charges between the iron and nitrogen atoms are −0.16 for ^{2}**1**, −0.08 for ^{2}**2** and −0.07 for ^{2}**3**. Hence, the higher intensity of the Fe–N band in **1** (Figure 1a) is rationalized by the relatively higher polarity of the Fe–N bond compared to complexes **2** and **3** (Figures 2a and 3a). The remaining unexplained difference between ^{2}**2** and ^{2}**3** has led us to inspect the normal vibrational modes. We observed a strong interconnection between the Fe–N stretch and ligand vibrations in 800–860 cm^{-1} region in ^{2}**3**. This results in two $^{14/15}$N-sensitive vibrations at 800 and 855 cm^{-1}. The first combination (at 800 cm^{-1}) is dominated by the ligand vibration. The large intensity of this band is probably due to a favourable ("constructive") sum of the Fe–N and ligand dipole

moment vectors along the vibrational mode. Conversely, the second combination has a dominant contribution from the Fe–N vibration and is associated with the small band intensity probably due to an unfavourable ("destructive") sum of the Fe–ligand/Fe–N dipole moment vectors along the vibrational mode. This is the reason why several bands in this region shift upon ^{15}N labelling and probably also why the Fe–N vibration in **3** has a very low intensity.

In conclusion, we detected Fe–N vibrations of three octahedral iron(V) nitrides. The Fe–N vibrations in two of the complexes are extremely weak, yet still possible to detect by helium tagging IRPD spectroscopy. The sensitive detection is possible because the method operates with isolated molecules in the gas phase at 3 K. We examined the electronic structure of the nitride complexes by CASPT2 calculations. The complexes have two quasi-degenerate doublet states with one unpaired electron in the antibonding π^*–d_{yz} and π^*–d_{xz} orbitals, and one low-lying doublet excited state with the unpaired electron in the $d_{x^2-y^2}$ orbital, being non-bonding with respect to the Fe–N bond. We showed that the effect of this complex electronic structure on the IR spectra can be predicted by experiment-calibrated DFT calculations. The calculations showed that the Fe–N band can almost vanish because of the interaction of the Fe–N stretching vibration with ligand vibrations. Therefore, the coupling of the electronic states and related vibrational coupling can make IR characterization of some Fe–N bonds challenging. The results further show that the experimental Fe–N stretching frequencies are insensitive to ligand architecture and charge of the complex and do not correlate with chemical behaviour: monocationic **1** is completely unreactive towards C=C bonds in the gas phase,[18] whereas dicationic **3** is highly reactive,[23] yet their Fe–N stretching vibrations lie at almost identical frequencies.

Acknowledgements

The project was supported by the European Research Council (ERC CoG No. 682275), the Czech Ministry of Education, Youth and Sports (LTAUSA17026), the Czech Science Foundation (15-10279Y) and the COST action ECOSTBio. M.S. is also grateful to the Czech Academy of Sciences for the Purkyně fellowship. M.C. acknowledges the financial support from the MINECO of Spain (CTQ2015-70795-P), the Catalan DIUE of the Generalitat de Catalunya (2009SGR637) and the ICREA-Academia award. The authors would like to thank Dr. Carlos V. Melo for proofreading the manuscript.

Conflict of interest

The authors declare no conflict of interest.

Keywords: ab initio calculations · hypervalent metal complexes · ion spectroscopy · iron(V) nitride · vibrational spectroscopy

[1] M. M. Abu-Omar, A. Loaiza, N. Hontzeas, *Chem. Rev.* **2005**, *105*, 2227–2252.
[2] a) B. Meunier, S. P. de Visser, S. Shaik, *Chem. Rev.* **2004**, *104*, 3947–3980; b) W. N. Oloo, L. Que, Jr., *Acc. Chem. Res.* **2015**, *48*, 2612–2621; c) X. Engelmann, I. Monte-Perez, K. Ray, *Angew. Chem. Int. Ed.* **2016**, *55*, 7632–7649; *Angew. Chem.* **2016**, *128*, 7760–7778.
[3] E. I. Solomon, K. M. Light, L. V. Liu, M. Srnec, S. D. Wong, *Acc. Chem. Res.* **2013**, *46*, 2725–2739.
[4] B. Mondal, L. Roy, F. Neese, S. Ye, *Isr. J. Chem.* **2016**, *56*, 763–772.
[5] J. F. Berry, *Comments Inorg. Chem.* **2009**, *30*, 28–66.
[6] J. E. M. N. Klein, L. Que, Jr., *Biomimetic High-Valent Mononuclear Nonheme Iron-Oxo Chemistry, in Encyclopaedia of Inorganic and Bioinorganic Chemistry* (Ed.: R. A. Scott, Wiley, Chichester, **2016**.
[7] E. Andris, R. Navrátil, J. Jašík, T. Terencio, M. Srnec, M. Costas, J. Roithová, *J. Am. Chem. Soc.* **2017**, *139*, 2757–2765.
[8] J. Torres-Alacan, P. Vöhringer, *Int. Rev. Phys. Chem.* **2014**, *33*, 521–553.
[9] J. J. Scepaniak, C. S. Vogel, M. M. Khusniyarov, F. W. Heinemann, K. Meyer, J. M. Smith, *Science* **2011**, *331*, 1049–1052.
[10] J. M. Smith, D. Subedi, *Dalton Trans.* **2012**, *41*, 1423–1429.
[11] J. Hohenberger, K. Ray, K. Meyer, *Nat. Commun.* **2012**, *3*, 720.
[12] W. D. Wagner, K. Nakomoto, *J. Am. Chem. Soc.* **1989**, *111*, 1590–1598.
[13] T. Petrenko, S. DeBeer George, N. Aliaga-Alcalde, E. Bill, B. Mienert, Y. Xiao, Y. Guo, W. Sturhahn, S. P. Cramer, K. Wieghardt, F. Neese, *J. Am. Chem. Soc.* **2007**, *129*, 11053–11060.
[14] J. F. Berry, E. Bill, E. Bothe, S. DeBeer George, B. Mienert, F. Neese, K. Wieghardt, *Science* **2006**, *312*, 1937–1941.
[15] W. R. Scheidt, S. M. Durbin, J. T. Sage, *J. Inorg. Biochem.* **2005**, *99*, 60–71.
[16] A. B. Wolk, C. M. Leavitt, E. Garand, M. A. Johnson, *Acc. Chem. Res.* **2014**, *47*, 202–210.
[17] J. Roithová, A. Gray, E. Andris, J. Jašík, D. Gerlich, *Acc. Chem. Res.* **2016**, *49*, 223–230.
[18] D. Schröder, H. Schwarz, N. Aliaga-Alcalde, F. Neese, *Eur. J. Inorg. Chem.* **2007**, 816–821.
[19] O. Krahe, F. Neese, M. Engeser, *ChemPlusChem* **2013**, *78*, 1053–1057.
[20] M. Schlangen, J. Neugebauer, M. Reiher, D. Schröder, J. Pitarch López, M. Haryono, F. W. Heinemann, A. Grohmann, H. Schwarz, *J. Am. Chem. Soc.* **2008**, *130*, 4285–4294.
[21] J. P. Boyd, M. Schlangen, A. Grohmann, H. Schwarz, *Helv. Chim. Acta* **2008**, *91*, 1430–1434.
[22] E. Andris, R. Navrátil, J. Jašík, G. Sabenya, M. Costas, J. Roithová, *Angew. Chem. Int. Ed.* **2017**, *56*, 14057–14060; *Angew. Chem.* **2017**, *129*, 14245–14248.
[23] G. Sabenya, L. Lázaro, I. Gamba, V. Martin-Diaconescu, E. Andris, T. Weyhermüller, F. Neese, J. Roithová, E. Bill, J. Lloret-Fillol, M. Costas, *J. Am. Chem. Soc.* **2017**, *139*, 9168–9177.
[24] N. Aliaga-Alcalde, S. DeBeer George, B. Mienert, E. Bill, K. Wieghardt, F. Neese, *Angew. Chem. Int. Ed.* **2005**, *44*, 2908–2912; *Angew. Chem.* **2005**, *117*, 2968–2972.
[25] a) M. Reiher, *Chimia* **2009**, *63*, 140–145; b) R. K. Szilagyi, M. Metz, E. I. Solomon, *J. Phys. Chem. A* **2002**, *106*, 2994–3007; c) J. N. Harvey, M. Aschi, *Faraday Discuss.* **2003**, *124*, 129–143; d) G. Schenk, M. Y. M. Pau, E. I. Solomon, *J. Am. Chem. Soc.* **2004**, *126*, 505–515.
[26] P. Pulay, *Int. J. Quantum Chem.* **2011**, *111*, 3273–3279.
[27] a) F. Neese, *Coord. Chem. Rev.* **2009**, *253*, 526–563; b) V. Polo, J. Grafenstein, E. Kraka, D. Cremer, *Theor. Chem. Acc.* **2003**, *109*, 22–35.
[28] Frequencies were obtained from the force constant k by formula $\tilde{\nu} = 1/(2\pi c)(k/\mu)^{1/2}$, where k is the force constant, μ is the reduced mass (11.2 amu for $^{56}Fe^{14}N$) and c is the speed of light.
[29] A. E. Reed, R. B. Weinstock, F. Weinhold, *J. Chem. Phys.* **1985**, *83*, 735–746.

Manuscript received: November 9, 2017
Accepted manuscript online: January 3, 2018
Version of record online: ■■ ■■, 0000

COMMUNICATION

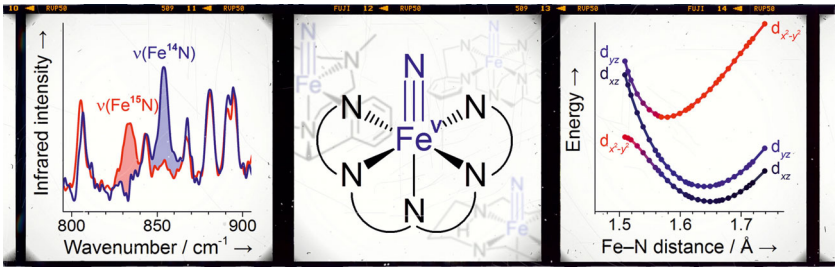

Seen at 3 K! Octahedral iron(V) nitrides have been resisting characterization by conventional vibrational spectroscopy. Now, we have accomplished their characterization in the gas phase, including the assignment of the Fe–N vibration. Their complicated electronic structure, uncovered by high-level ab initio calculations, results in masking of the Fe–N stretching vibration.

Hypervalent Complexes

E. Andris, R. Navrátil, J. Jašík, G. Sabenya, M. Costas, M. Srnec,* J. Roithová**

■■ – ■■

Detection of Indistinct Fe–N Stretching Bands in Iron(V) Nitrides by Photodissociation Spectroscopy